

Hydrocephalus Shunt Valve

BME 301

April , 2017

Team: Emma Alley (Leader), Andrew Miller (Communicator/BPAG), Karl Fetsch (BWIG), Catharine Flynn (BSAC)

Advisor: Beth Meyerand

Client: John Webster

Abstract

Hydrocephalus is a condition affecting three in every 2000 individuals at birth, and is the most common cause for brain surgery in children and infants [1]. High intracranial pressures caused by hydrocephalus are alleviated by the implantation of a shunt valve. Shunt valves designed to remove cerebrospinal fluid (CSF) from the interior of the blood-brain barrier have been used to treat hydrocephalus since the inception of spring-controlled valves in the 1960s [2]. Shunt valves have since evolved with the diversification of biomaterials and micro-scale electronics. However, complications with overdrainage, underdrainage, and siphoning continue to plague the designs, frustrating researchers and medical experts alike. Even with the development of highly advanced, programmable differential pressure systems, top of the line shunt valves display failure rates of 81% within 12 years of implantation [3]. The proposed device incorporates the use of localized ambient pressure and that within the brain as the primary means of regulating fluid flow and control of the siphon effect. CSF removal is dictated *via* the incorporation of a Kelvin-Voight model of viscoelasticity to avoid commonly observed complications associated with overdrainage of fluid. We hypothesize that the model proposed will more optimally control intracranial CSF levels in comparison to market-standard, differential pressure-based systems.

Table of Contents

Table of Contents	1
1. Introduction	2
1.1 Motivation and Project Impact	2
1.2 Existing Devices/Competing Designs	3
1.3 Problem Statement	4
2. Background	4
2.1 Biology and Physiology	4
2.2 Design Specifications	6
2.3 Client Information	7
3. Preliminary Designs	7
3.1 Dual Membrane Design	7
3.2 Dashpot Design	8
3.3 Door-Flap Design	9
3.4 Punctured Dome Design	10
4. Preliminary Design Evaluation	11
4.1 Evaluation of the Design Matrix	11
4.2 Proposed Final Design	12
5. Fabrication	13
5.1 Materials	13
5.2 Fabrication	13
5.3 Final Prototype	14
6. Testing	15
7. Results	17
8. Discussion	18
9. Conclusions	20
10. Acknowledgements	21
11. References	21
12. Appendix	23

1. Introduction

1.1 Motivation and Project Impact

Hydrocephalus is an incredibly common condition that affects three in every 2000 individuals at birth and is the most common reason for brain surgery in children and infants. If left untreated, hydrocephalus can cause failure of suture fusion of the skull plates, brain damage, or even death. The total average medical expenditures on hydrocephalus exceed \$1 billion per year, yet current research is limited: the National Institutes of Health invests less than \$1 million in the subject per year. Over 40,000 operations are conducted annually to attempt to correct the symptoms of hydrocephalus. Approximately 30% of these operations are the patient's first corrective surgery, which often includes the implantation of a valve to shunt CSF away from the cerebrospinal space when pressure becomes too high. [1] This suggests that the majority of operations are performed to correct shunt valve failures. Failure to properly treat individuals, such as when a shunt valve malfunctions, can result in brain damage: roughly 30% of individuals with hydrocephalus will experience intellectual disability at some point in their life. [4]

1.2 Existing Devices/Competing Designs

There are currently a multitude of valve options offered to patients suffering from hydrocephalus. Unfortunately, there has yet to be a shunt valve brought to market that has the potential to serve as a 'universal' treatment option. Specific components that may aid in the functionality of the device in a particular individual can present as the cause of failure when the same device is implanted into a different individual. Patients generally consult with their neurologists in order to determine the type of valve that will function most optimally in their case. Additionally, small changes can be implemented by the neurosurgeon mid-operation to better fit the valve to the needs of the individual.

Shunt valves designed for hydrocephalic patients are designated to one of six subtypes based on the type of pressure by which the valve operates as well as the inclusion/exclusion of additional flow regulating components. These six valve subtypes are defined as: fixed differential pressure (DP), fixed DP with anti-siphon mechanisms, programmable DP, programmable DP with anti-siphoning mechanism, programmable anti-siphoning mechanism, and purely mechanical ambient pressure. Each of the first four valve subtypes listed function *via* reading changes in pressure across the valve, between outflow port and inflow port. A 'fixed' valve indicates the valve operates using an absolute pressure threshold, above which the valve opens and drainage can occur [5]. This requires surgeons and doctors to accurately anticipate the drainage needs of the individual pre-surgery to avoid the need of subsequent operations to adjust the pressure threshold of the valve. With modern advancements in micro-scale technology,

programmable pressure valves have been developed to eliminate the need for multiple operations by the integration of electrical components that allow doctors to adjust pressure thresholds from outside the body. A common mode of failure observed in these valves is the formation of a blockage at the junction of tubing and the valve itself, a phenomena commonly referred to as proximal occlusion. Proximal occlusion has been observed to be indirectly related to problems with valve overdrainage due to creation of a siphoning effect [3]. To alleviate the extent that overdrainage occurs, newly presented shunt designs have begun to incorporate the use of flow regulating devices to control for the siphoning effect (anti-siphoning mechanisms) and gravity compensation devices to account for complications that occur from changes in altitude such as flying or standing up [6]. However, the use of such flow regulating components have been associated with insufficient drainage in obese individuals.

New research efforts have begun to shift the focus of shunt valve designs away from using differential pressure as the mechanism that dictates opening and closing of the device [7,8]. Rather, research suggests ambient pressure in the brain can serve as a reliable alternative. It is hypothesized that the construction of a valve relying on a differential between ambient and inflow pressure (as opposed to inflow and outflow pressure) could assist in control of the siphoning effect while still draining sufficient amounts of fluid to avert potential trauma due to increased intracranial pressure.

1.3 Problem Statement

A shunt valve controlling the expulsion of cerebrospinal fluid (CSF) from inside the blood-brain barrier to the abdomen in patients suffering from hydrocephalus is needed. The device will be of a minute enough size to avoid irritation in patients when implanted underneath the chin or behind the ear. Additionally, the device will avoid using electronic-based valve mechanisms, functioning on a purely mechanical basis. This is to avoid encountering circuitry problems as well as electronic failure. CSF is released from the skull of the patient by tubing, flowing through the tubing to the device. Flow is blocked by the valve until sufficient pressure opens the valve to drain the CSF into the abdomen where it is reabsorbed.

2. Background

2.1 Biology and Physiology

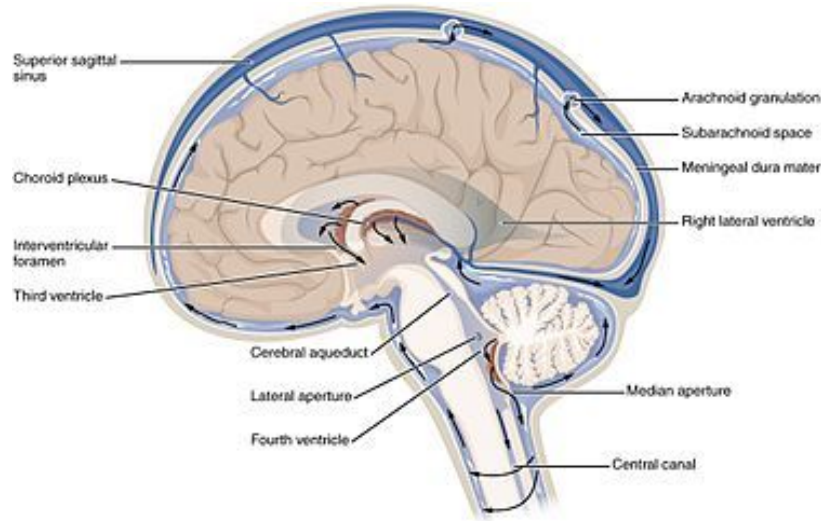


Figure 1: The image depicts the flow of CSF through the skull and spinal column. The section labeled “cerebral aqueduct” is equivalent to the aqueduct of sylvius

(https://en.wikipedia.org/wiki/Cerebrospinal_fluid#/media/File:1317_CFS_Circulation.jpg).

The condition hydrocephalus is caused by the insufficient drainage of cerebrospinal fluid from the skull [9]. The CSF under normal intracranial pressures acts a delivery system for nutrients, a garbage disposal system for waste, and a protective coating against impact between the brain and the skull. The CSF is generated within the choroid plexuses (situated within the ventricles), which are the locations of diffusion across the blood-brain barrier. The flow of CSF starts in the lateral ventricles, moves into the third ventricle, then to the fourth via the aqueduct of sylvius and final out into circulation around the brain and spinal cord (Fig. 1). After the nutrients within the CSF have been consumed and replaced with waste, it is reabsorbed by the arachnoid granulations within the meninges to be recycled by the body [10]. CSF in a hydrocephalus patient generally accumulates within the ventricles, causing the intraventricular pressure to build, forcing the brain to expand into the skull, and crushing it if fluid cannot escape (Fig. 2) [11].

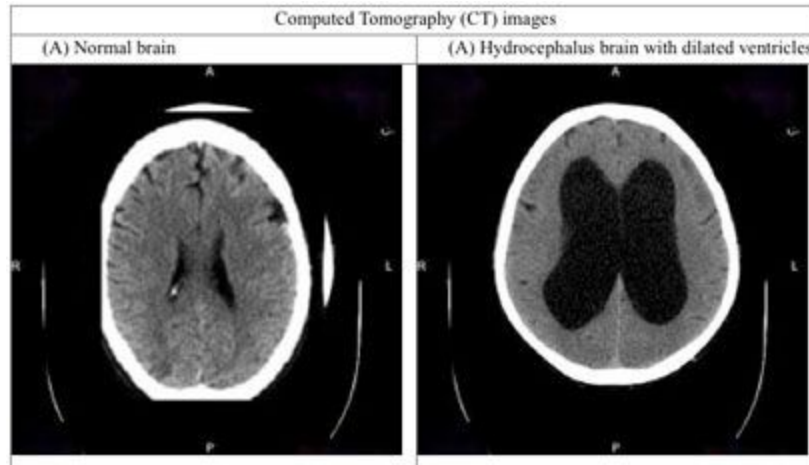


Figure 2: The two CT scans depict a normal brain (left) compared to one with hydrocephalus (right). The brain with hydrocephalus has severely dilated lateral ventricles (<http://www.barnabashealth.org/images/MMC/MMC-Neuroscience/hydrocephalus-1.jpg>).

Typically, the inhibition of adequate flow of CSF that leads to hydrocephalus occurs before CSF is transported out of the fourth ventricle, with the aqueduct of sylvius being to most common site of blockage, however there are many causes for the condition. In the case of congenital hydrocephalus, which refers to those born with the condition, often times birth defects lead to stenosis of cerebral aqueducts, the spaces between ventricles. Infants can be born with naturally small aqueducts, however sometimes other defects can result in hydrocephalus [9]. Spina bifida, a birth defect that occurs when one or more of the vertebra do not properly form, results in an opening that the spinal cord can protrude from in the back. The displacement of the spinal cord can cause a herniation of the hindbrain through the foramen magnum (location where the skull and vertebrae join), and block the flow of CSF through the fourth ventricle resulting in hydrocephalus [9,12].

Acquired hydrocephalus refers to the acquisition of the condition after birth. The age range for individuals who can acquire hydrocephalus ranges from infancy to late adulthood, due to the various causes of the disease. Meningitis, multiple sclerosis, trauma, stenosis, sclerosis of aqueducts, and tumor growth are all potential causes of acquired hydrocephalus [9,13].

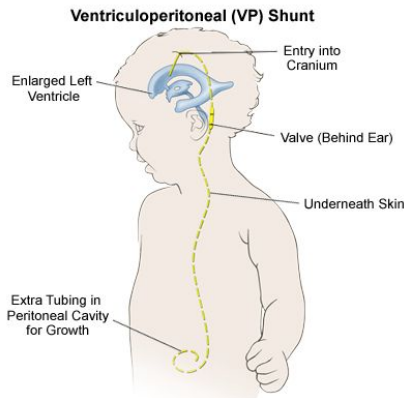


Figure 3: The image shows a child who has had a valve implanted. The ventricles are denoted in blue, and the catheter shunt system are yellow (<https://www.roshreview.com/wp-content/uploads/Image-VP-ventriculoperitoneal-shunt.png>).

Generally, treatment for hydrocephalus requires brain surgery (Fig. 3). A catheter is placed into the lateral ventricles, and it exits via the back of the skull, remaining under the skin. The catheter is then snaked behind the ear, where the shunt valve is placed. The end of the valve is connected to another catheter, which drains the CSF to the abdomen.

2.2 Design Specifications

All components must be biocompatible, as an implanted device must not negatively interact with the body or be degraded by normal physiological processes. Moving parts need to have resistance to repeated strain with the overall system having an increased lifespan (more than 12 years). The system should not allow interaction between CSF and interstitial fluids. The client has stipulated that the design must operate based on an intracranial/ambient pressure differential (as opposed to an intracranial/abdominal pressure differential). Moreover, it should avoid repeated openings and closings as a result of rapid pressure changes from the heartbeat. It must safely remove CSF fluid when ICP is higher than acceptable without over draining. Any openings the valve has to the interstitial space should be less than or equal to $3\mu\text{m}$ in diameter to prevent tissue ingrowth. No electronic or magnetizable components should be included in the design. Finally, the valve should be smaller than a US half-dollar coin ($\sim 30\text{ mm}$ in diameter, $\sim 2\text{ mm}$ in thickness).

2.3 Client Information

Prof. John G. Webster works in the Biomedical Engineering department at UW Madison, and works jointly with Prof. Joshua Medow from the Dept. of Neurological Surgery to develop instruments for patients with hydrocephalus. He is currently working on an instrument capable of

externally reading intracranial pressure from an internal sensor implanted in the head. He is also working on a device capable of alleviating patients with sleep apnea.

3. Preliminary Designs

The most feasible designs brought up during the brainstorming process are discussed. The designs were comparatively evaluated using the design matrix shown in section IV.

3.1 Dual Membrane Design

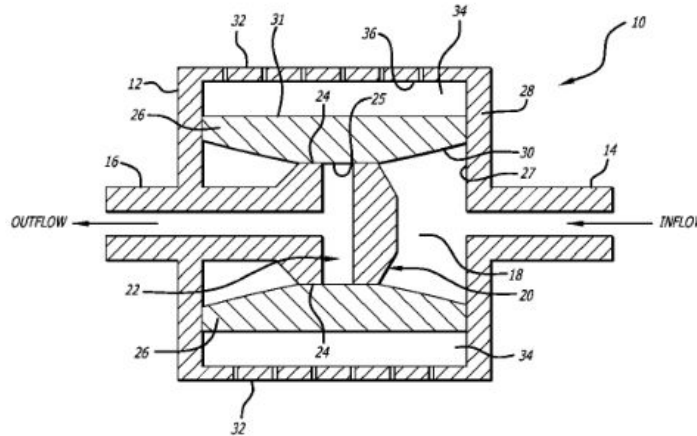


Figure 4: Differential pressure valve. Inflow pressure pushes against ambient pressure to open and close the valve (<https://www.google.com/patents/US9526879>).

The first design discussed is a patent from 2016 intended to operate as an ambient pressure-controlled hydrocephalus shunt valve (Fig. 4). Fluid flows in from the brain in the inflow into the large chamber and exerts an outward pressure on the two flexible membranes. The membranes in turn are forced inwards by the surroundings. When inflow pressure is greater than ambient pressure, the two membranes flex outward and fluid flows into the T-shaped junction, and leaves as the outflow. The benefit of this design is that it prevents overdrainage: when the valve is already closed, sudden spikes in negative outflow pressure (e.g. from standing up) do not result in overdrainage since there is no way for fluid to be sucked in from the inflow [7]. Disadvantages of this design include concerns with tissue ingrowth into the spaces between the outer walls and flexible membranes and the fact that the design is already patented. This could obviously inhibit efforts to modify the design and adapt it for the team's requirements.

3.2 Dashpot Design

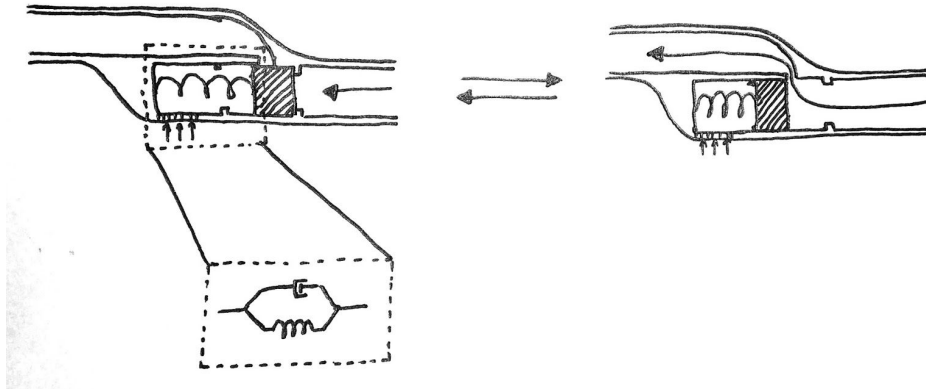


Figure 5: Spring-Dashpot operated valve. Valve is opened by inflow pressure, the movement of which is resisted by the dashpot element (by Karl Fetsch).

The second design discussed is intended to smooth out the pressure coming from the brain and consists of a valve that opens and closes with behavior resembling a dashpot and spring in parallel (Fig. 5). The valve blocks an opening and seals the CSF inflow from the brain. A spring opposes the force from the CSF. When the fluid pressure increases, the valve slowly moves backwards, with speed controlled by the dashpot element. This element in its current form consists of a membrane with several holes that allows incompressible fluid to **slowly** move through. This design would prevent sudden spikes in pressure from forcing the valve open, which could increase the lifetime of the design by preventing fatigue. Additionally, since the drainage opening is located to the side of the drainage valve, there is no possibility of overdrainage when the valve is closed, since the negative pressure would be exerted perpendicular to the valve's movement. Potential problems with this design include the possibility of fluid leakage around the valve element and unwanted biological effects of the dashpot membrane sucking in and extruding fluid from/into the interstitial space.

3.3 Door-Flap Design

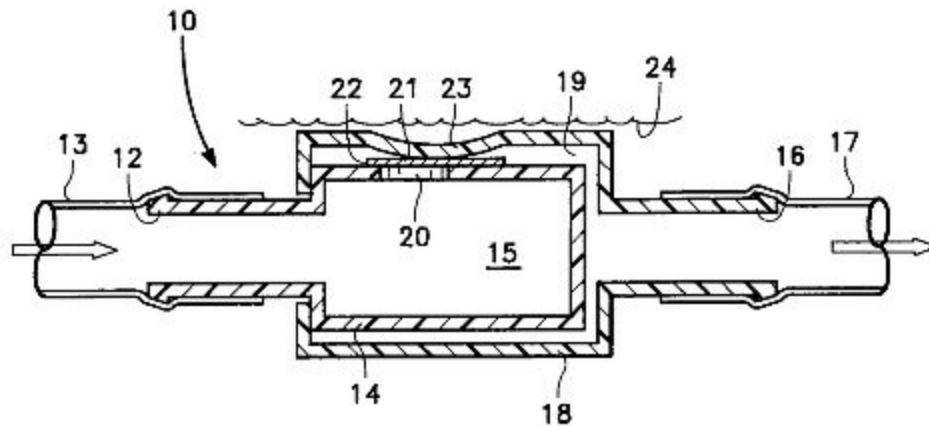


Figure 6: Ambient pressure operated valve. Inflow pressure acts against ambient pressure to operate the opening and closing of a small flap, which seals the drainage hole (<https://www.google.ch/patents/US20040082900>).

The third design examined was another patent for an ambient pressure valve (Fig. 6). This design operates similarly to the dual membrane design, but instead of using empty spaces between membranes and a flexible material to close the drainage opening, a flexible membrane directly exposed to the surroundings moves a small flap to seal and open the drainage hole. CSF would flow into the chamber and exert pressure on the flap, which would be opposed by ambient pressure. When inflow pressure surpasses ambient pressure, the flap opens and fluid flows out [8]. Like the first design, there is no chance for overdrainage since negative pressure has no way of affecting the system. However, expected problems with this design include the manufacturability of the small parts and the potential for fatigue on the small, delicate flap. It is also an already patented design, bringing into question the feasibility of the team working with it.

3.4 Punctured Dome Design

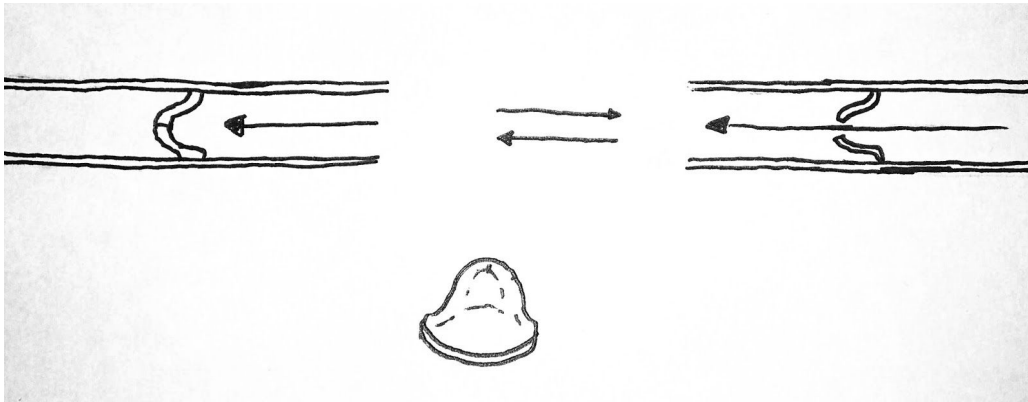


Figure 7: Differential pressure valve. Inflow pressure deforms the flexible material, expanding a small hole in the tip, allowing drainage (by Karl Fetsch).

The final design considered was a very simple differential pressure valve, consisting of a flexible dome-shaped piece with a small hole at the apex (fig. 7). When pressure behind the valve gets to a certain point, it is forced open and fluid drains. Problems expected included the possibility of overdrainage and fatigue from repetitive opening and closing.

4. Preliminary Design Evaluation

The team evaluated the preliminary designs based on the design matrix (Table 1).

Table 1. Design Matrix

Properties (Weight)	Dual Membrane	Dashpot	Door-Flap	Dome
Cost (5)	4	3	4	5
Ease of Fabrication (20)	3	3	4	5
Safety (15)	4	4	3	2
Longevity (20)	4	5	3	2
Accuracy/ Precision (25)	4	4	3	2
Manufacturability (10)	3	4	3	5
Size (5)	3	3	4	5
Total (100)	73	78	65	64

4.1 Evaluation of the Design Matrix

The following sections denote the properties of each criterion, their respective weighting, and the designs that scored notably well or poorly by the specifications that the team set forth.

Cost (5/100): This criterion is based on the cost of fabrication during the prototyping phase. The weight of this is low compared to the other criteria because all designs were presumed to be under budget and have similar large-scale production costs. The Dome Design scored the highest in this category, as it required the least amount of materials to fabricate.

Ease of Fabrication (20/100): A highly weighted criteria, this was based on the team’s ability to create a large scale prototype with current fabrication skills. Once again, the Dome Design was scored the highest in this category due to its simplicity.

Safety (15/100): Safety is a moderately weighted criterion based on the required materials’ interaction with the body at the implantation site as well as consideration of how prone

the device could be to failure *in vivo*. The Dashpot and Dual Membrane designs tied with the highest scores in this category because they prevent backflow.

Longevity (20/100): Tied for the second most heavily weighted criterion with Ease of Fabrication, it considers the perceived length of time the device can operate in the body without change in the mechanical properties. The Dashpot Design was projected to suffer the least amount of wear because the dashpot resists sudden applications of force, imparting a longer lifetime. Thus, it scored the highest in the Longevity category.

Accuracy/Precision (25/100): The ability of the system to drain fluid in an accurate manner, only draining the CSF when the intracranial pressure is above the upper threshold and preventing drainage before the intracranial pressure is under the lower threshold. The Dashpot and Dual Membrane design scored the highest in this category as the predictability of their mechanical properties made them more customizable.

Manufacturability (10/100): Manufacturability considers the perceived ease to manufacture the design in an industrial setting. This was weighted relatively low because this criterion is beyond the scope that the team can achieve within the allotted project time frame. The team still considered this criterion because the ultimate goal is to create a design that could be manufactured and sold on the market as an effective alternative to hydrocephalus valves currently in use. The Dome Design scored the highest in this criterion due to the simplicity of its design.

Size (5/100): The criterion describes the overall size of the final design that would be implanted within the body. It was scored relatively low because the final designs should be similar in their sizes. The ultimate factor that was considered was the relative complexity of the designs, where more parts would result in a larger device. The Dome Design scored the highest in this category as it had the smallest design.

4.2 Proposed Final Design

Although there are some possible issues with leakage and biological interactions, the spring-dashpot operated design was selected for further work. This selection was made based on its ability to smoothly regulate the intracranial pressure and to avoid problems with overdrainage commonly seen with standard differential-pressure shunt valves. High scores in perceived longevity and precision categories were the driving forces behind design selection.

5. Fabrication

Due to the budgeting constraints of this project, the team opted to fabricate a large-scale demonstrative prototype over a fully functional to-scale prototype. The design was fabricated entirely from off-the shelf materials for the same reason.

5.1 Materials

The budget for this project was set by the client at \$100 for all materials and fabrication. A full list of materials used in this project along with associated costs can be found in the project's expense sheet, located in appendix B of this report.

PVC piping, end caps, brushing and an adaptor piece were purchased from a local hardware store and used to construct the outer housing of the valve. The piping piece stores the piston along with the incoming CSF. End caps are used to store the spring and creates the lower fluid reservoir for incoming interstitial fluid. PVC brushing can be adhered to the piping portion and is the female companion to a barbed nylon adaptor piece that creates the inflow port and fits to the inflow tubing.

A 1" diameter ultra-high molecular weight polyethylene (UHMWPE) dowel rod was purchased from MSC direct (part #52432481) and was machined to create the valve's piston. AS568a-020 rubber O-rings were purchased from Hydraulic Warehouse and fitted to the piston to create a dynamic seal that prevented leakage of CSF into the lower fluid reservoir. The steel spring contained within the lower reservoir assists the interstitial fluid in providing adequate counterforce to the CSF in the upper reservoir. The spring was immobilized on the end cap and the brushing attached to the piping piece through use of an EP-200 epoxy putty adhesive.

5.2 Fabrication

The piston head was lathed from the PE rod in the student shop after a 5 inch piece was cut using the drop saw. A 0.05 inch thin bit was used to cut the o-ring grooves. A 0.15 inch drill bit followed the center drill to make a space for the spring's guide rod. The hole was flattened and sized further with the flat bore. The surfaces were finished by lightly passing over the surface with the basic cutting tool. The length of the piston was cut from the rod using the parting tool. The remaining nipple on the piston was removed using the basic cutting tool and finished with the same tool. The part was filed carefully in the lathe. A SolidWorks rendering of the model can be seen in Fig. 8. An engineering drawing with dimensions used to fabricate the piston can also be found in appendix D (p. 41).

The O-ring sizes were selected based off of a set of O-ring equations and sealing guidelines found online, found in appendix B.1 [13]. Based on this, the team selected 1" OD x 7/8" ID O-rings to fit a 1" bore diameter in the valve housing.



Figure 8. SolidWorks model of valve in cutaway of housing (by Andrew Miller).

5.3 Final Prototype

A single prototype was fabricated with the help of Andrew Wild. Several changes were made to the final proposed design. For one, the prototype was significantly scaled up, due to budget constraints and the difficulties of precisely fabricating a small scale model. For the same reasons, the biocompatibility design criteria was ignored, and the team focused on using cheap and easy-to-acquire off-the-shelf parts. However, this should not be an issue for future work as every material has a biocompatible analogue. Holes were added to the underside of the end cap piece to create fluid union between the outer environment and lower fluid reservoir of the shunt. The size of these holes also function as the dashpot-like element of the design. Given their small diameter; short, rapid spikes in fluid pressure are hindered from causing piston displacement and accidental overdrainage. Finally, the team incorporated the use of O-rings on the piston, as previous designs did not include them and had experienced problems with leakage. The final prototype is seen in fig. 9.

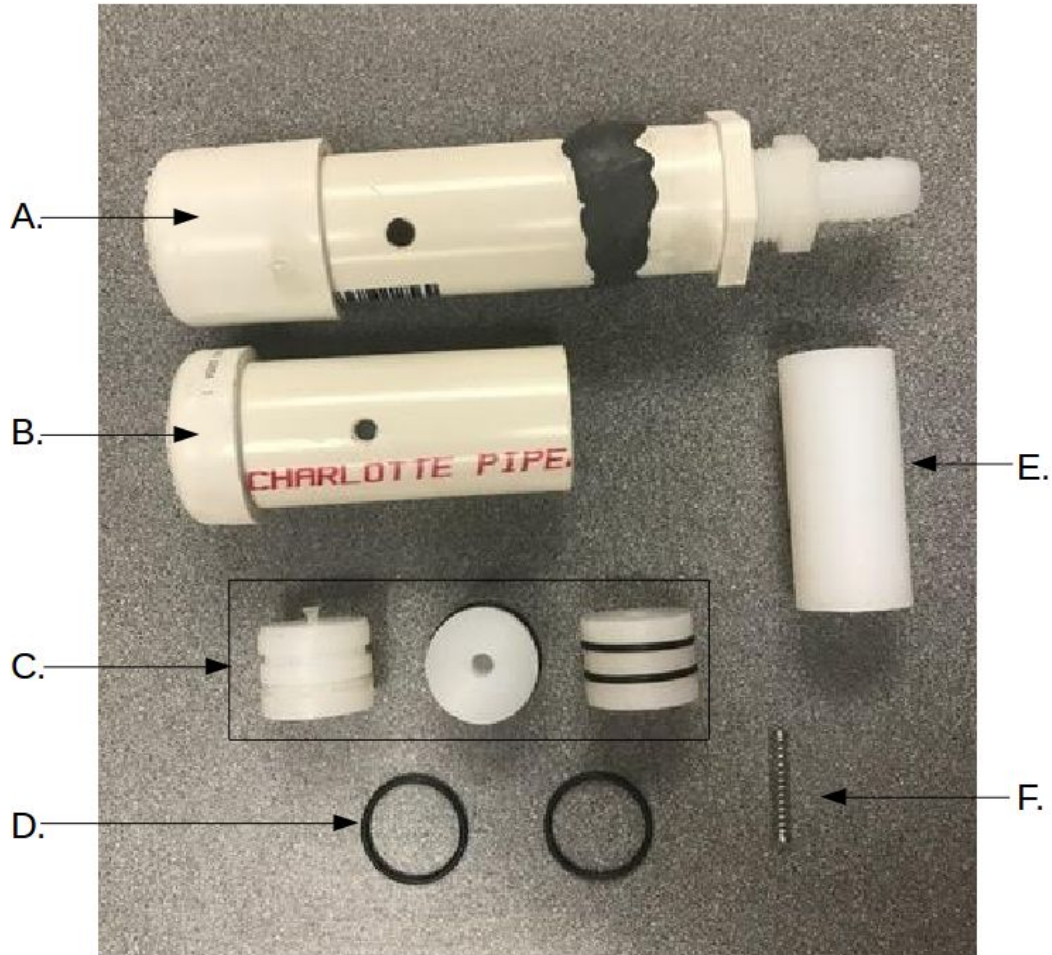


Figure 9. Collection of prototypes and parts used for fabrication. A. Final prototype. B. Tube with spring and valve used for mechanical testing. C. Piston prototypes; these were made with incorrect dimensions but display the basic idea and placement of O-rings. D. O-rings. E. Uncut section of PE dowel used for valve fabrication. F. Spring, similar to the one used in the final prototype (by Emma Alley).

6. Testing

Piston and spring parts were tested on the MTS Criterion - C43. Refer to section VII for a report of the results of the tests performed. Data was exported to MatLab for evaluation.

Spring Testing

Initial spring testing was performed to evaluate the efficacy of two springs to return the force applied upon them (i.e. the spring constant, k). The program used was the BME 315 3-point bending and the springs were each displaced approximately 4 mm. The spring constants were calculated in Matlab using the line of best fit. Results for this test are found in appendix C.

Piston Testing

The piston was tested in housing B, utilizing the spring with the higher k value. The two testing conditions were water lubricated and dry chamber, or water-filled lower chamber. The piston was lubricated by running the valve under water and shaking out excess water. The lower chamber was filled by partially immersing the housing in a 100 mL beaker filled with water, as seen in figure 10. Water entered into the chamber through holes on the end cap.



Figure 10. Example of set up for piston testing while the lower chamber was filled with water. Lubricated testing was performed similarly but the piston was lubricated with water and not immersed in water (by Andrew Miller).

The piston was tested for maximum force to completely open the valve. Valve open-ness was qualitatively evaluated as the piston was compressed (using the BME 315 3-point bending program) and the test was manually stopped. The valve was deemed completely open when the o-ring passed the the bottom of the outlet. The crosshead was then returned to the original position to perform another test. Three tests were performed consecutively for each condition. The maximum value for each of the trial was evaluated to establish an average value, and data was processed using MatLab and excel (see appendix C to reference MatLab code).

Cyclic load testing was performed to evaluate the recovery of the piston. “Good file” BME 315 3-point cyclic load testing program was used to perform this test. The piston was compressed to 5.75 mm and then returned to the original position. The test was performed three times consecutively for each of the lubricated and immersed conditions. The percent energy returned was evaluated in MatLab.

7. Results

Compression testing

Force-displacement graphs for one sample of each tested condition were plotted alongside one another using MatLab for a visual comparison of each system's response to axial loading (Fig. 11A). Calculations from data acquired during MTS testing yielded average max compression forces of $10.419 \text{ N} \pm .488 \text{ (SE) N}$ and $10.557 \text{ N} \pm 0.164 \text{ N}$ for the water-lubricated ($N=3$) and immersed conditions ($N=3$), respectively (Fig. 11B). Max compression force to fully open the valve was not found to be significantly different between the two conditions ($\alpha=0.05$, $t(4) = -0.267$, $p = 0.803$, two-tailed). Thus, inclusion of fluid in the valve's lower reservoir did not significantly contribute to the force required to fully open the valve.

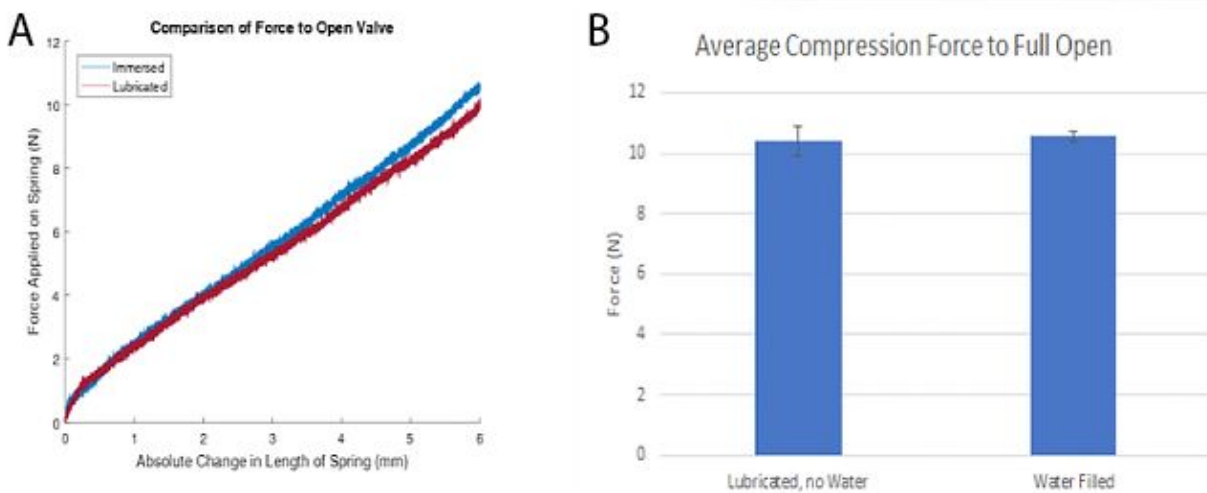


Figure 11. Results of MTS compression testing of the shunt valve prototype. Testing was performed until a displacement of 6 mm occurred and the associated force value was recorded for a lubricated condition ($N=3$) and a water-immersed condition ($N=3$). (A) Force-displacement curve generated using Matlab in which the full compression of the piston was plotted from one sample at each condition (by Catharine Flynn). (B) Bar graph representing the average force to fully open the piston at each of the specified conditions (by Andrew Miller). Columns represent mean values with error bars representing ± 1 SE.

Cyclic Load Testing

Force-displacement graphs for one sample of each tested condition were plotted alongside one another using Matlab for a visual comparison of each system's response to cyclic loading (Fig. 12A). Calculations for percent energy returned were acquired by division of energy during loading by energy during the unloading phase. Cyclic loading revealed average percent energy returns of $53.593 \% \pm 1.068 \text{ (SE) } \%$ and $60.423 \% \pm 0.483 \%$ for the water-lubricated ($N=3$) and immersed conditions ($N=3$), respectively (Fig. 12B). Percent energy returned to the system following a fully loaded and unloaded cycle was found to be significantly different

between the two conditions ($\alpha=0.05$, $t(4)= -5.83$, $p= 0.004$, two-tailed). The team’s interpretation of this result was that the inclusion of fluid in the valve’s lower reservoir significantly contributes to the valve’s ability to recover energy following loading.

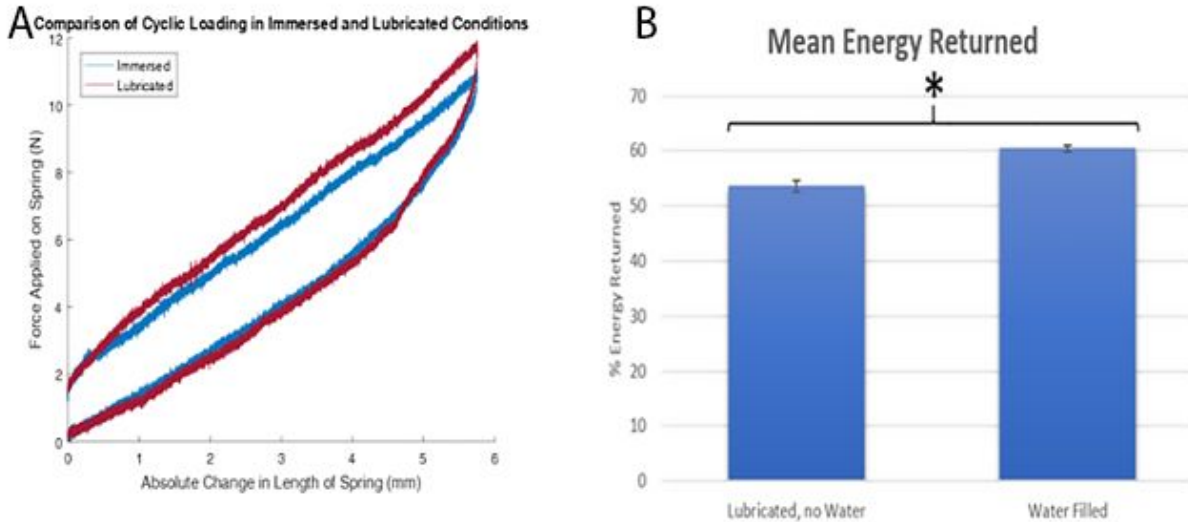


Figure 12. Results of MTS cyclic load testing of the shunt valve prototype. Loading was performed until a displacement of 5.75 mm occurred. The unloading phase was then carried out until the crosshead returned to its initial position and the associated percent energy returned was calculated for a lubricated condition ($N=3$) and a water-immersed condition ($N=3$). (A) Force-displacement curve generated using Matlab in which the cyclic loading of the piston was plotted (one sample of each condition) (by Catharine Flynn). (B) Bar graph representing the mean energy returned to the system at each of the specified conditions (by Andrew Miller). Columns represent mean values with error bars representing ± 1 SE. (*) denotes treatment means were statistically different.

8. Discussion

Initial testing of the prototype showed that while some aspects of ambient pressure improved the functionality of the valve, it did not completely contribute to expectations. The significance of the cyclic loading test ($p=0.004$) shows that the inflow of the ambient fluid does contribute to energy return of the system, as it returned more energy ($60.423 \% \pm 0.483 \%$) than the non-immersed control ($53.593 \% \pm 1.068\%$). The results indicate that the use of ambient pressure and fluids can contribute positively to the overall system of the valve, though the returned energy is significantly lower than the ideal energy return of 100%. This could be contributed to fabrication error, as the device was not manufactured by professionals. The fabrication of the slits are most likely the cause of this error, as the O-rings in the system could have been too wide for the tube causing a higher friction coefficient, thus decreasing the springs ability to return to its neutral positions.

The compression testing experiment showed somewhat less promising results than the cyclic loading test. Overall, the force required to compress the piston to the fully open position for the immersed ($10.557 \text{ N} \pm 0.164 \text{ N}$) and water-lubricated ($10.419 \text{ N} \pm .488 \text{ N}$) samples was insignificant ($p= 0.803$). The results indicate that the ambient pressure did not play a factor in increasing the overall pressure required to displace the piston to the fully open position. Factors that may have contributed to the insignificance of the ambient pressure may have been that the friction forces as well as the forces provided by the spring were so much larger than ambient pressure that it hardly contributed in comparison. In addition, the semi-permeable membrane that allowed for fluid inflow and outflow may have been too large, effectively allowing fluid to displace with less resistance. Another possible error within this experiment may be attributed to the sight of immersion. The fluid filled beaker was not a closed system meaning fluid that was displaced out of the bottom of the valve was able to flow into a non-pressurized container. This differs from how fluid displacement would function within the body, as the body is a closed system and the tissues would act more elastically, similar to a balloon [15].

Many assumptions were made in order to model the shunt valve system. One of the assumptions was that CSF and water shared the same viscosity. In actuality, the viscosity of water and CSF are not the same, however when temperatures are varied the water can work as a viable substitute. CSF can vary in viscosity per individual depending on protein concentrations, however the average viscosity of CSF at 37°C is roughly $1.003 \text{ g/m}^*\text{s}$ [16]. In comparison water at 37°C is $0.692 \text{ g/m}^*\text{s}$. Because the viscosity of water is much different than that of CSF at body temperature, the system would need to be cooled in order to more accurately portray viscosity. Water viscosity at 20°C has a similar viscosity to CSF, measuring at $1.002 \text{ g/m}^*\text{s}$. The tests were run at 22°C , thus water had a viscosity of $0.955 \text{ g/m}^*\text{s}$ [17]. The experimental procedure could have seen increased accuracy with further cooling of the testing water. The use of CSF or accurate CSF analogues at 37°C was not possible for the purposes of these experiments due to a limited budget.

Another assumption was made on the basis that the shunt valve model would be scaleable. However, with current results, it would appear that changes will need to be made to the current model to enable scalability. The spring and friction forces currently contribute too much to the existing system. In the case of implantation within the body, the ICP would be expected to range between 5-15 mm Hg and the ambient pressure between 1.92-6.55 mm Hg, implying that the ambient pressure should be contributing approximately half of the needed pressure in order to keep the piston at rest [18, 19]. However, the current shunt valve model, as dictated from the compression testing results, would indicate that ambient pressure plays almost no role in keeping the piston at rest. In order to evaluate this, investigations into smaller spring constants and decreasing the amount of friction experienced by the O-rings would need to be performed.

9. Conclusions

Hydrocephalus is a common and serious condition that can result in brain damage, arising when there is insufficient drainage of cerebrospinal fluid from the cranium. Currently the only known treatment to alleviate this condition is the implantation of a valve that shunts CSF fluid out of the cranium when the pressure becomes too high. Current shunt valves rely on a pressure differential between the CSF and the pressure within the abdomen. These designs are plagued with problems such as overdrainage, which occurs when there is a spike in negative pressure in the abdomen, causing the valve to open and drain fluid when it should not. Valves currently have a failure rate of 80% within 12 years of implantation, unacceptable for a device that should have a lifetime survivability. The goal of this project was to create a design that operates on an intracranial/ambient pressure differential, in hopes that ambient pressure variations will more safely operate the valve.

The dashpot-piston design was selected due to its ability to ‘smooth’ out the pressure spikes from the cranium. It operates based on the ambient-intracranial pressure differential, which in practice should prevent overdrainage. The dashpot will prevent the design from opening from random pressure spikes. Using off the shelf parts such as PVC piping, rubber O-rings, a polyethylene rod, and a spring, the team constructed a large scale proof of concept, with the intent of scaling down in future studies.

Compression testing of the piston revealed that water within the fluid reservoir did not significantly change the force required to compress the piston ($p = 0.803$). During cyclic testing of the piston, it was found that inclusion of fluid in the valve’s lower reservoir significantly contributes to the valve’s ability to recover energy following loading ($p = 0.004$). The heightened energy returned by the system is desirable, and indicates that the presence of ambient pressure did have a positive regulatory impact on the operation of the device.

Challenges the team faced with this design included inexperience with fabrication and limited budget. These challenges manifested themselves in the final design, which did not have biocompatibility and was much too large. In addition, the final prototype had fluid leakage despite the presence of O-rings. Both of these issues could be accounted for in future work, given a higher budget and more careful machining techniques.

Future work on the design could include changes to the dashpot fluid reservoir in order to close it off from the surrounding interstitial fluid, or alternatively experimenting with replacing the dashpot and spring with a biocompatible viscoelastic polymer that would retain the spring-dashpot behavior and also be able to transmit ambient pressure to the piston. Additionally, it is vital that mathematical models of the physical operation of the design are made, in order to scale it down. It will also be necessary to compare the accuracy of these equations to the

real-world behavior of the valve. Finally, the design should be tested in more physiologically relevant conditions, e.g. using a fluid whose viscosity mirrors that of CSF rather than just using water.

10. Acknowledgements

The team would like to thank Dr. John Webster for providing us with the design problem and offering his assistance throughout the semester. We would also like to thank Prof. Beth Meyerand for her guidance and moral support. Finally we would like to thank Andrew Wild in the ECB machine shop for his assistance and guidance with prototype fabrication.

11. References

- [1] "Facts and Stats | Hydrocephalus Association", *Hydroassoc.org*, 2017. [Online]. Available: <http://www.hydroassoc.org/about-us/newsroom/facts-and-stats-2/>. [Accessed: 21- Feb- 2017].
- [2] H. Solomon, "Hydrocephalus Shunt with Spring Biased One-Way Valves." U.S. Patent 3,288,142 A, issued November 29, 1996.
- [3] Sainte-Rose C, Piatt J, H, Renier D, Pierre-Kahn A, Hirsch J, F, Hoffman H, J, Humphreys R, P, Hendrick E, B, Mechanical Complications in Shunts. *Pediatr Neurosurg* 1991/1992;17:2-9. 21 Jan. 2017.
- [4] "Facts about Hydrocephalus | Hydrocephalus statistics | NHFOnline.org", *Nhfonline.org*, 2014. [Online]. Available: <http://nhfonline.org/facts-about-hydrocephalus.htm>. [Accessed: 21- Feb- 2017].
- [5] Drake, James M., et al. "Randomized trial of cerebrospinal fluid shunt valve design in pediatric hydrocephalus." *Neurosurgery* 43.2 (1998): 294-303.
- [6] Portnoy, Harold D., et al. "Anti-siphon and reversible occlusion valves for shunting in hydrocephalus and preventing post-shunt subdural hematomas." *Journal of neurosurgery* 38.6 (1973): 729-738.
- [7] D. Watson, "Shunt Valve for Controlling Siphon Effect." US Patent 9,526,879 B2, issued Dec. 27, 2016.
- [8] E. D. Luttich, "Proportional Control Device for a Hydrocephalus Shunt." U.S. Patent 20,040,082,900 A1, applied April 29, 2004.

- [9] McAllister, "Pathophysiology of congenital and neonatal hydrocephalus", *Seminars in Fetal and Neonatal Medicine*, vol. 17, no. 5, pp. 285-294, 2012.
- [10] "Cerebrospinal Fluid (CSF)", *National Multiple Sclerosis Society*, 2017. [Online]. Available:
[http://www.nationalmssociety.org/Symptoms-Diagnosis/Diagnosing-Tools/Cerebrospinal-Fluid-\(CSF\)](http://www.nationalmssociety.org/Symptoms-Diagnosis/Diagnosing-Tools/Cerebrospinal-Fluid-(CSF)). [Accessed: 21- Feb- 2017].
- [11] "Hydrocephalus - Mayo Clinic", *Mayo Clinic*, 2017. [Online]. Available:
<http://www.mayoclinic.org/diseases-conditions/hydrocephalus/basics/definition/con-20030706>. [Accessed: 21- Feb- 2017].
- [12] S. Leibold, A. Keefover-Hicks, C. Wilson, D. Dulworth, S. Collins, T. Pensabene-Lewis, R. Talbott and J. Anderson, "Identifying Nursing Interventions Related To Spinal Fusion Surgery In The Child With Spina Bifida", *International Journal of Nursing in Intellectual & Development Disabilities*, vol. 5, no. 13, 2017.
- [13] Alfred Hospital, "Obstructive hydrocephalus caused by multiple sclerosis.", Prahran, 1989.
- [14] "Design Guidelines for Radial Seals," EfunDa, 2017 [Online]. Available:
http://www.efunda.com/designstandards/oring/design_guidelines.cfm. [Accessed April 2017].
- [15] Chen, J. Novakofski, W. Jenkins and W. O'Brien, "Young's modulus measurements of soft tissues with application to elasticity imaging", *IEEE Transactions on Ultrasonics, Ferroelectrics and Frequency Control*, vol. 43, no. 1, pp. 191-194, 1996
- [16] A. Linninger, M. Xenos, D. Zhu, M. Somayaji, S. Kondapalli and R. Penn, "Cerebrospinal Fluid Flow in the Normal and Hydrocephalic Human Brain", *IEEE Transactions on Biomedical Engineering*, vol. 54, no. 2, pp. 291-302, 2007.
- [17] B. González, N. Calvar, E. Gómez and Á. Domínguez, "Density, dynamic viscosity, and derived properties of binary mixtures of methanol or ethanol with water, ethyl acetate, and methyl acetate at T=(293.15, 298.15, and 303.15)K", *The Journal of Chemical Thermodynamics*, vol. 39, no. 12, pp. 1578-1588, 2007
- [18] E. Crisan, J. Chawla. "Ventricles of the Brain". Medscape. Editor: S.R. Benbadis. June 30, 2016. [<http://emedicine.medscape.com/article/1923254-overview>]
- [19] S. Kelly and P. Macklem, "Direct measurement of intracellular pressure.", *Am J Phys Cell Phys*, vol. 10, no. 33, pp. 652-657, 2017.

12. Appendix

A. Product Design Specifications: Hydrocephalus Shunt Valve

February 2, 2017

Team: Emma Alley (Leader), Andrew Miller (Communicator/BPAG), Karl Fetsch (BWIG), Catharine Flynn (BSAC)

Advisor: Beth Meyerand

Client: John Webster

Function

The valve device controls the expulsion of cerebrospinal fluid (CSF) from inside the blood-brain barrier to the abdomen in patients suffering from hydrocephalus. The device will be of a minute enough size to avoid irritation in patients when implanted beneath the chin or behind the ear. Additionally, the device is to stray away from currently applied electronic-based valve mechanisms, functioning purely mechanically. This is to avoid encountering circuitry problems as well as electronic failure. CSF is released from the skull of the patient through a catheter inserted into the ventricles of the brain. The device blocks flow until a sufficient pressure opens the valve. CSF is drained into the abdomen where it is reabsorbed.

Client requirements

- Prevent debris from entering system
- Self-regulating
 - Maintain a form of homeostasis with ambient pressure
 - Openings in shunt allow it to regulate with surrounding tissue
 - Openings in shunt to environment will be $\leq 3\mu\text{m}$
 - Placed under flaccid skin (either behind chin or ear)
 - No electronic components
- Address increased pressure due to heartbeat
- Increase longevity of device

Design requirements

- Biocompatibility (all components)
- Resistance to repeated strain (relevant components)
- Flexibility or rigidity (depending on component)

- Sealed (does not allow leakage outside the catheter system)
- Does not become clogged by tissue ingrowth
- Responds to changes in ambient **and** intracranial pressures--must safely remove CSF fluid when necessary without over draining
- Small size (described as about the size of a half dollar coin)

1. Physical and Operational Characteristics

- Performance requirements:** The device will need to last a lifetime, because ideally after implantation, it will never need to be removed. The shunt should also be able to remove excess fluid from the skull at approximately 1 ml/min, and should be designed so tissues do not clog the valve within the shunt. In order to properly displace excess pressure in the skull, the device should be designed to incorporate the use of ambient pressure as opposed to differential pressure. This will remove many complications patients suffer when standing up or changing elevations (such as in air travel).
- Safety:** The device poses two main safety concerns if it is improperly designed: over draining and under draining of cerebrospinal fluid from the skull. Over drainage can cause a significant drop in intracranial pressure, and in extreme cases, leading to the collapse of the ventricles in the brain due to insufficient support. In the reverse scenario, under drainage increases intracranial pressure, increased size of the ventricles push the brain out, damaging the tissues [1]. Almost all of the ways that the device would fail, would cause one of these two scenarios to occur if untreated.
- Accuracy and Reliability:** Current devices have a failure rate of about 40%, so the proposed design needs to be more reliable than the standard for shunt valves. This lowered failure rate must be retained throughout the entire life of the product, corresponding with the patient's lifespan. The shunt should not need to be removed. Shunts will also need to be flexible in design, so that they may be customized for each patient's unique physiology.
- Life in Service:** Each shunt should be designed so that it may last the lifetime of the patient. In order to have the required longevity, the device needs to be designed to include ambient pressure as opposed to differential pressure. Differential pressure based shunts tend to cause complications with common actions, such as standing up too quickly or riding on airplanes.
- Shelf Life:** The device will be made out of polymers or biocompatible metals, so the storage life will be limited by the methods of sterilization. If the device can be re-sterilized before implantation, the shelf life should be indefinite.

- f. **Operating Environment:** The device will function in standard human physiological conditions and fail to instigate an immune response. Such physiological conditions include a pH of 7.4 and temperature of approximately 37 degrees Celsius. The device will need to withstand pressure on all faces from the forces CSF will be exerting on the device's internal walls. Additionally, the final product must be resistant to failure as a result of tissue ingrowths. The device should prevent backflow through the valve and provide resistance to rapid opening and closing resulting from sudden pressure fluctuations such as heartbeats and changes due to standing or altitude.
- g. **Ergonomics:** A common problem with competing shunt valves is the disconnection of tubing and migration of the valve from the original implantation site. To avoid this issue, the device must be completely immobilized within tissue. Further, the device must also not allow for tissue ingrowth to occur to an extent that function is lost. Since the device is idealized to remain in the patient for the remainder of his/her life, the device must be composed of materials resistant to biodegradation. Though infection is highly unlikely to occur with commonly used biomaterials, special caution may need to be taken with the implantation occurring in close proximity to the skull and brain.

With regard to device function, multiple factors must be considered with respect to ergonomics. The valve must be able to withstand the hydrostatic pressure of the CSF it contains, pressures from surrounding tissues, and other biological material on the outer walls. Fracture is the most common source of failure in hydrocephalus shunt valves and a tough material is required to avoid this pitfall. The device will also need to operate with the pressure ranges from CSF in the human brain. The entire function of the shunt valve will be anticipated to rely on CSF reaching a certain pressure threshold, at which time the valve opens and pressure is relieved.

- h. **Size:** The design is estimated to be comparable to a half dollar, circular with a diameter of approximately 32 mm. The thickness is speculative, but is likely to be less than 20 mm. The principal concern for reducing the size is the patient's comfort.
- i. **Weight:** The weight will likely be under 10g. The principal concern for reducing the weight is for the patient's comfort.
- j. **Materials:** All materials used in the final product should be biocompatible (i.e. not degrade or cause immune reactions in the body). Furthermore, the materials used should be able to withstand repetitive loading and unloading without changes to their physical properties or breaking. Finally, magnetic metals need to be avoided since hydrocephalus is a condition that often requires MRIs.

For our purposes, because we ended up creating a proof of concept model, not all of the materials in our final prototype were biocompatible. The materials used in our design that would need to be substituted for biocompatible parts in a final product were the PVC casing, the EP-200 Epoxy Putty, and the O-rings. The PVC could be replaced with silicon and the O-rings could be replaced with a neoprene substitute.

- k. Aesthetics, Appearance, and Finish:** Finish of material should be smooth to reduce patient discomfort and to allow for optimal flow of fluid through the device. Outward superficial aesthetics are not a concern as the device is an implant, however, the valve ought to be visibly labeled for implantation ease.

2. Production Characteristics

- a. Quantity:** Only one working prototype needs to be produced for demonstrative purposes.
- b. Target Product Cost:** The budget for this project was \$100, and was provided by the client. Total expenditures were around \$60 (including the purchasing of tools for fabrication) and the materials cost per part was \$10.08.

3. Miscellaneous

- a. Standards and Specifications:** The FDA has set forth requirements for Neurological devices under 21 CFR § 882.5550. Hydrocephalus Shunts are considered to be a Class II medical device (21 CFR § 860.3(c)), needing to demonstrate effectiveness and safety (21 CFR § 860.7). The FDA recognizes ISO 7192 (2006) and ASTM F647 (2014) relating to Hydrocephalus Shunts.
- b. Customer:** Customers will be considered to be the implanting surgeons and the patients who use the valve. The valve should not be noisy for the patient (no repetitive clicking for example). The device should also be as small as possible to complete its function so that the patient can live a relatively normal life after implantation.
- c. Patient-related concerns:** As mentioned in the ‘operating environment’ section, there is serious risk of shunt valve failure in patients with hydrocephalus. Research studies have shown upwards to 81% of shunt valve implants fail within their twelve years of implantation. Additionally, failure of the first implant increases risk of failure in subsequent implants [2]. Patients receiving these valve implants must understand these associated risks of failure when being provided treatment options.

Another important concern for patients is that no valve mechanisms proposed to date have shown to be a unanimous best option for all. Devices containing anti-siphoning mechanisms to prevent backflow and overdrainage are highly suggest for tall, slender

individuals whereas these devices can result in underdrainage in obese individuals. Thus, there is no universal shunt valve design and patients should perform individual research and consult their health professional when considering implants.

- d. Competition:** The first designs for shunt valves appear to come from the 1960s in which one-way spring valves were used in an attempt to provide a novel drainage system to move collecting CSF in the brain into an absorbable area such as the abdomen [3]. Current hydrocephalus shunt valves operate using a variety of components. Some devices consist of fixed differential pressures valves that will open and close at predetermined values while others can be programmed from outside the body to different limits. In order to prevent a siphon effect, anti-siphoning devices such as the ball and cone mechanisms are often used. There are also new patent designs in which the valve operates purely mechanically with no need for electronics [4]. It appears these new biomaterial-inspired designs could overcome many of the shortcomings of current programmed shunt valves. The common theme amongst all researched shunt valves shows a device in which an upper and lower pressure limit is set, similar to a filter mechanism. When the upper threshold is reached in terms of differential pressure, the device opens and CSF is moved through the outflow pipe. When pressure falls back below the lower limit the valve closes and overdrainage is avoided.

References

- [1] "Complications Of Shunt Systems | Hydrocephalus Association". *Hydroassoc.org*. N.p., 2017. Web. 2 Feb. 2017.
- [2] Sainte-Rose C, Piatt J, H, Renier D, Pierre-Kahn A, Hirsch J, F, Hoffman H, J, Humphreys R, P, Hendrick E, B, Mechanical Complications in Shunts. *Pediatr Neurosurg* 1991/1992;17:2-9. 21 Jan. 2017.
- [3] Salomon, Hakim. Hydrocephalus Shunt with Spring Biased One-way Valves. Salomon Hakim, assignee. Patent US3288142 A. 29 Nov. 1966.
- [4] Watson A, David. Shunt Valve for Controlling Siphoning Effect. David Watson, assignee. Patent US9526879 B2. 27 Dec. 2016.

B. Materials List and Expenses

- AS568a-020 O-rings
- PVC piping: 1.25'' OD x 1'' ID
- PVC piping end cap: 1.50'' OD x 1.25'' ID
- Steel spring

- PVC bushing: 1'' ID x 1.25'' OD
- Adaptor piece
- EP-200 epoxy putty
- 1'' diameter UHMWPE dowel rod

Expense Sheet

Date:	Item:	Cost/per (quantity purchased); Total cost:	Comments (all materials purchased out of pocket unless otherwise noted):
4/09/17	Nitrile Gloves	\$2.27/pack (2x); \$4.54 total	For safety handling PVC cement
4/09/17	Nylon Barb	\$2.15/piece (2x); \$4.30 total	Nozzle for inflow catheter attachment
4/09/17	PVC Brushing	\$1.09/piece (2x); \$2.18 total	Adapter piece cemented to PVC pipe; companion component to nylon barb
4/09/17	PVC Cap Slip	\$0.79/piece (4x); \$2.37 total	End cap; spring housing/ lower fluid reservoir
4/09/17	PVC Cement	\$4.33/pack (1x); \$4.33 total	Adhesive for PVC components
4/09/17	Epoxy Putty (2 oz.)	\$3.81/pack (1x); \$3.81 total	Adhesive for non-PVC components
4/09/17	Dust Masks	\$2.48/pack (2x); \$4.96 total	Safety handling carcinogenic adhesives
4/09/17	1"x2' PVC Pipe	\$2.26/piece (1x); \$2.26 total	Outer housing
4/11/17	1"x4' UHMWPE dowel	\$11.43/piece (1x); \$11.43 total	Piston piece (Purchased through BME department from MSC direct)
4/11/17	1"OD x 7/8"ID x 1/16" O-rings	\$0.10/ring (10x); \$4.98	Fluid sealant
		Total: \$45.16	

B.1 O-Ring Selection

O-ring dimensions were selected based on a series of guidelines found on [efunda.com](http://www.efunda.com). Starting with a bore diameter (Bd) of 1 inch, the team selected to use AS568a-020 O-rings with ID of 7/8" and OD of 1". These would fit over a groove diameter (Gd) of 0.8938". This would give an O-ring stretch value of 0.0210 (nearly exactly the recommended value) and a compression below the maximum recommended value. All equations and tables adapted from http://www.efunda.com/designstandards/oring/design_guidelines.cfm.

$$ID = G_d (1 - S_{rec})$$

$$CS > \frac{B_d - G_d}{2}$$

$$GW = CS(1.5)$$

ID=Inner Diameter, Gd=Groove Diameter, S_{rec}=Recommended Stretch, CS=Cross Section, Bd=Bore Diameter, GW=Groove Width

Operating Point	O-Ring Stretch Value	
	%	S
minimum	1%	0.01
maximum	5%	0.05
recommended	2%	0.02

Seal Type	Recommended Maximum Compression	
	%	C
static	40%	0.40
dynamic	30%	0.30

C. MatLab Code

The code is followed by the respective output.

C.1. Spring Constant Testing

The x_1 value is the spring constant in N/mm.

```
%% Spring Constant Testing
% v 1.5
% April 27, 2017
% BME 301: shunt_valve
% Author: Catharine Flynn
% Team Members: Emma Alley, Karl Fetsch, Drew Miller
% Let's do the time warp again!

%% clear command window, close all windows, clear workspace
clc;
close all;
clear;

%% Summary of Test Parameters
% * testFile.data(:,1) Crosshead, the displacement of the MTS head (mm)
% * testFile.data(:,2) Load (N)
% * testFile.data(:,3) Time(s) The function (uimport) automatically
% sorts out the data from the header text. If not, the user can do that
% instead.

%% Import data
% f = fullfile('myfolder','mysubfolder','myfile.txt')
% (subfolder may be omitted) I needed to change the names of the testing
% files. The ellipsis, dash and multiple spaces are now gone. This allows
% for zip file compression of the folder. Unfortunately, every file needed
% to be changed--as did the code. My life. 'DAQ- Crosshead, ... -
% (Timed).txt' -> 'DAQ- Crosshead, (Timed).txt'

% data for short spring
datum = fullfile('SpringTesting', 'CompressionTest1', 'DAQ- Crosshead,
(Timed).txt');
structSpringA = uimport(datum);
% data for tall spring
datum = fullfile('SpringTesting', 'TensionTest1', 'DAQ- Crosshead,
(Timed).txt');
structSpringB = uimport(datum);

%% Equalize data set lengths
% We're moving everything up by the smallest number in the two data sets to
% avoid number problems later on: the size of the matrices need to be the
% same to be graphed properly, can easily use axis to graph the data
x = min(size(structSpringA.data(:,1)), size(structSpringB.data(:,1)));

dblDispA = structSpringA.data(1:x,1);
dblLoadA = structSpringA.data(1:x,2);
dblDispB = structSpringB.data(1:x,1);
```

```

    dblLoadB = structSpringB.data(1:x,2);

%% calculate lines of best fit
% finds coefficients of polynomial and error estimation structure for a 1
degree polynomial
[pSpringA, structSpringAStat] = polyfit(dblDispA,dblLoadA,1);
% generates data points corresponding to the line of best fit, delta contains
50% of the predictions for future x
[ySpringA, deltaSpringA] = polyval(pSpringA,dblDispA, structSpringAStat);

[pSpringB, structSpringBStat] = polyfit(dblDispB,dblLoadB,1);
[ySpringB, deltaSpringB] = polyval(pSpringB,dblDispB, structSpringBStat);

%% Plot data
figure;
hold on;    % plots everything on the same figure
    % plot data
    plot(dblDispA,dblLoadA,'-b', dblDispB,dblLoadB,'-r');

    %plot lines of best fit

    % plot(dblDispA(1:100:x), ySpringA(1:100:x),'Marker', '-.', 'Color', [0.88,
0.89, 0.97], 'LineWidth', 1, dblDispB,ySpringB,'-.k','LineWidth', 1,);
    % vector(startIndex:jumpEveryNValue:stopIndex)
    % Did this so the line is dotted. Can also be used to graph fewer data
    % points quickly. 'MarkerIndices' has the same visual effect as the
    % commented out version but it makes sure that the x and the y vectors
    % are both the same length. (In the other version both vectors are
    % manipulated to prevent errors when generating the graph.)

    plot(dblDispA, ySpringA,'LineStyle', '-.', 'Color', [0.8, 0.898, 1],
'LineWidth', 2);
    % it is so much easier to just change the color and the line width than
    % to the extensive nonsense on line 64
    plot(dblDispB, ySpringB,'-.k','LineWidth', 2);

    % headings
    xlabel('Absolute Change in Length of Spring (mm)');
    ylabel('Force Applied on Spring (N)');
    title('Evaluation of Load vs Spring Behavior');

    % legend
    legend('Spring A', 'Spring B', 'Line of Best Fit, Spring A', 'Line of Best
Fit, Spring B', 'Location','northwest');

    % fit bounds to data
    axis tight;
hold off;
%% Statistics of Lines of Best Fit
mdlSpringA = fitlm(dblDispA,dblLoadA, 'linear', 'RobustOpts','on')

```



```
mdlSpringB = fitlm(dblDispB,dblLoadB, 'linear', 'RobustOpts','on')
```

```
mdlSpringA =
```

```
Linear regression model (robust fit):
```

```
y ~ 1 + x1
```

```
Estimated Coefficients:
```

	Estimate	SE	tStat	pValue
(Intercept)	0.53369	0.0015545	343.32	0
x1	1.2585	0.00070341	1789.2	0

```
Number of observations: 11483, Error degrees of freedom: 11481
```

```
Root Mean Squared Error: 0.0833
```

```
R-squared: 0.996, Adjusted R-Squared 0.996
```

```
F-statistic vs. constant model: 3.2e+06, p-value = 0
```

```
mdlSpringB =
```

```
Linear regression model (robust fit):
```

```
y ~ 1 + x1
```

```
Estimated Coefficients:
```

	Estimate	SE	tStat	pValue
(Intercept)	0.037236	0.0016034	23.224	1.2539e-116
x1	0.48722	0.00072648	670.66	0

```
Number of observations: 11483, Error degrees of freedom: 11481
```

```
Root Mean Squared Error: 0.086
```

```
R-squared: 0.975, Adjusted R-Squared 0.975
```

```
F-statistic vs. constant model: 4.5e+05, p-value = 0
```

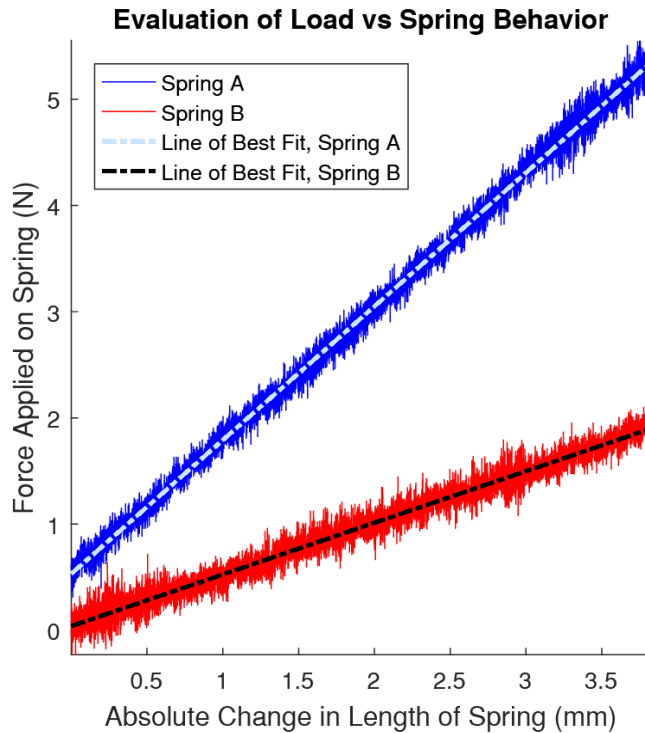


Figure 13. Graphical output of spring constant testing (by Catharine Flynn).

C.2. Maximum Force Testing

Two separate code files were created: one evaluating the data points while the piston housing was partially immersed in water and the other evaluating the data while the piston was lubricated with water. The two programs are extremely similar and only vary in the folders needed to access the data and the color scheme chosen to represent the data sets to better differentiate the outputs. While the program only outputs one figure of data, it was considered to be best to have both graphs for clarity.

```

%% Force to Fully Open Piston while Lubricated with Water
% v 0.1
% April 27, 2017
% BME 301: shunt_valve
% Author: Catharine Flynn
% Team Members: Emma Alley, Karl Fetsch, Drew Miller
% Muhahahahaha

%% clear command window, close all windows, clear workspace
clc;
close all;
clear;

%% Summary of Test Parameters
% * testFile.data(:,1) Crosshead, the displacement of the MTS head (mm)

```

```

% * testFile.data(:,2) Load (N)
% * testFile.data(:,3) Time(s) The function (uimport) automatically
% sorts out the data from the header text. If not, the user can do that
% instead.

%% Import data
% dat = fullfile('myfolder','mysubfolder','myfile.txt')
% (subfolder may be omitted, can also use unlimited subfolders)
% 'DAQ- Crosshead, ... - (Timed).txt' -> 'DAQ- Crosshead, (Timed).txt'

datum = fullfile('ForceToOpenImmersed', 'dunkForce1', 'DAQ- Crosshead,
(Timed).txt');
structTest1 = uimport(datum);

datum = fullfile('ForceToOpenImmersed', 'dunkForce2', 'DAQ- Crosshead,
(Timed).txt');
structTest2 = uimport(datum);

datum = fullfile('ForceToOpenImmersed', 'dunkForce3', 'DAQ- Crosshead,
(Timed).txt');
structTest3 = uimport(datum);

%% Assign variables
dblDisp1 = structTest1.data(:,1);
dblLoad1 = structTest1.data(:,2)+abs(structTest1.data(1,2));

dblDisp2 = structTest2.data(:,1);
dblLoad2 = structTest2.data(:,2)+abs(structTest2.data(1,2));

dblDisp3 = structTest3.data(:,1);
dblLoad3 = structTest3.data(:,2)+abs(structTest3.data(1,2));

%% Plot data
figure;
hold all; % plots everything on the same figure

% set colors for trials
color = [ 0 0.4470 0.7410
0.4940 0.1840 0.5560
0.3010 0.7450 0.9330];
set(groot,'DefaultAxesColorOrder', color)

% plot data
plot(dblDisp1, dblLoad1);
plot(dblDisp2, dblLoad2);
plot(dblDisp3, dblLoad3);

% headings
xlabel('Absolute Change in Length of Spring (mm)');

```

```

ylabel('Force Applied on Spring (N)');
title('Evaluation of Force to Open Valve while Chamber filled with Water');

% legend
legend('Trial 1', 'Trial 2', 'Trial 3', 'Location','northwest');

% fit bounds to data
axis([0 max(dblDisp3) 0 12]);
hold off;

%% Evaluate data
max1 = max(dblLoad1(1:length(dblLoad1)))
max2 = max(dblLoad2(1:length(dblLoad1)))
max3 = max(dblLoad3(1:length(dblLoad1)))

[h,p,ci,stats] = ttest([max1,max2,max3])

```

Output for Immersion Testing:

```

max1 =
    11.5593

max2 =
    11.8156

max3 =
    10.5497

h =
     1

p =
    0.0012

ci =
     9.6456    12.9708

stats =
    struct with fields:
        tstat: 29.2652
         df: 2
         sd: 0.6693

```

Output for Lubricated Testing:

```

max1 =
     9.5765

max2 =
    11.1046

max3 =
    11.1892

h =
     1

p =
    0.0024

ci =
     8.3687    12.8781

stats =
    struct with fields:
        tstat: 20.2728
         df: 2
         sd: 0.9076

```

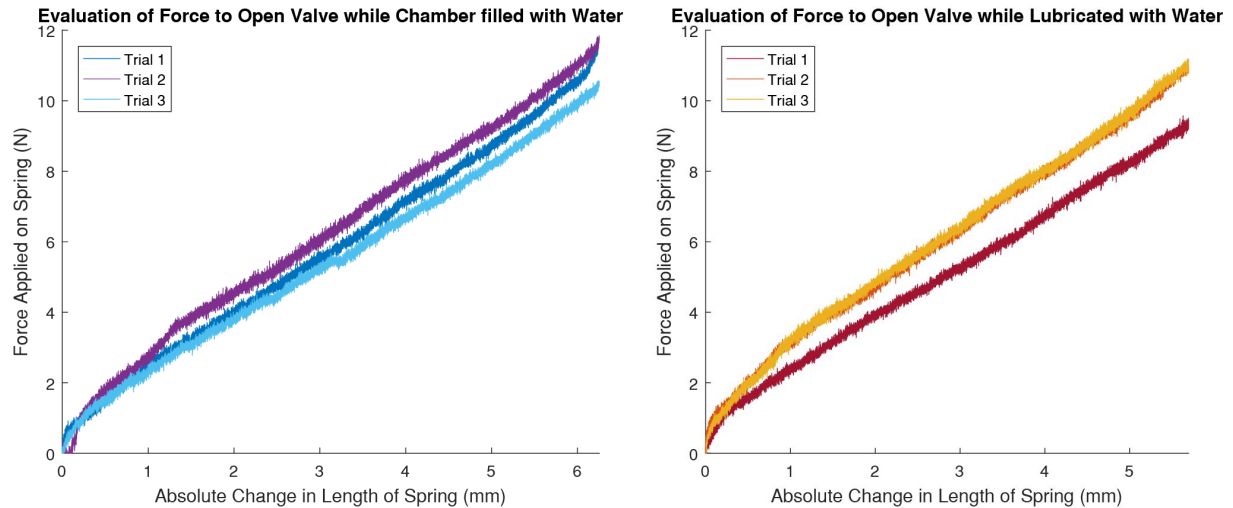


Figure 14. Graphs comparing maximum force required to fully open the valve. The graph for immersion testing is on the left and the graph for lubricated testing is on the right (by Catharine Flynn).

C.3. Cyclic Load Testing

Two separate code files were created: one evaluating the data points while the piston housing was partially immersed in water and the other evaluating the data while the piston was lubricated with water. The two programs are extremely similar and only vary in the folders needed to access the data and the color scheme chosen to represent the data sets to better differentiate the outputs. While the program only outputs one figure of data, it was considered to be best to have both graphs for clarity.

```

%% Cyclic Loading of Immersed Piston
% v 0.0
% April 27, 2017
% BME 301: shunt_valve
% Author: Catharine Flynn
% Team Members: Emma Alley, Karl Fetsch, Drew Miller
% By now, you can probably tell that I always write original code.

%% clear command window, close all windows, clear workspace
clc;
close all;
clear;

%% Summary of Test Parameters
% * testFile.data(:,1) Crosshead, the displacement of the MTS head (mm)
% * testFile.data(:,2) Load (N)
% * testFile.data(:,3) Time(s) The function (uuiimport) automatically
% sorts out the data from the header text. If not, the user can do that
% instead.

%% Import data

```

```

% dat = fullfile('myfolder','mysubfolder','myfile.txt')
% (subfolder may be omitted, can also use unlimited subfolders)
% 'DAQ- Crosshead, ... - (Timed).txt' -> 'DAQ- Crosshead, (Timed).txt'

% each test has two files
% increasing
datum = fullfile('CyclicImmersed', 'dunkCycle1', 'DAQ- Crosshead,
(Timed).txt');
structTest11 = uimport(datum);
% decreasing
datum = fullfile('CyclicImmersed', 'dunkCycle1', 'DAQ- Crosshead,
(Timed)1.txt');
structTest12 = uimport(datum);

% increasing
datum = fullfile('CyclicImmersed', 'dunkCycle2', 'DAQ- Crosshead,
(Timed).txt');
structTest21 = uimport(datum);
% decreasing
datum = fullfile('CyclicImmersed', 'dunkCycle2', 'DAQ- Crosshead,
(Timed)1.txt');
structTest22 = uimport(datum);

% increasing
datum = fullfile('CyclicImmersed', 'dunkCycle3', 'DAQ- Crosshead,
(Timed).txt');
structTest31 = uimport(datum);
% decreasing
datum = fullfile('CyclicImmersed', 'dunkCycle3', 'DAQ- Crosshead,
(Timed)1.txt');
structTest32 = uimport(datum);

%% Create variables for Test Cycle 1
x = min(size(structTest11.data(:,1)), size(structTest12.data(:,1)));
Crosshead11 = structTest11.data(1:x,1);
Load11 = abs(min(structTest12.data(1:x,2))) + structTest11.data(1:x,2);
Crosshead12 = structTest12.data(1:x,1);
Load12 = abs(min(structTest12.data(1:x,2))) + structTest12.data(1:x,2);

%% Create variables for Test Cycle 2
x = min(size(structTest21.data(:,1)), size(structTest22.data(:,1)));

Crosshead21 = structTest21.data(1:x,1);
Load21 = abs(min(structTest22.data(1:x,2))) + structTest21.data(1:x,2);
Crosshead22 = structTest22.data(1:x,1);
Load22 = abs(min(structTest22.data(1:x,2))) + structTest22.data(1:x,2);

%% Create variables for Test Cycle 3
x = min(size(structTest31.data(:,1)), size(structTest32.data(:,1)));

```

```

Crosshead31 = structTest31.data(1:x,1);
Load31 = abs(min(structTest32.data(1:x,2))) + structTest31.data(1:x,2);
Crosshead32 = structTest32.data(1:x,1);
Load32 = abs(min(structTest32.data(1:x,2))) + structTest32.data(1:x,2);

%% Plot data
figure;
hold all;    % plots everything on the same figure

% edit colors of tests for clarity
color = [    0    0.4470    0.7410
          0    0.4470    0.7410
          0.4940    0.1840    0.5560
          0.4940    0.1840    0.5560
          0.3010    0.7450    0.9330
          0.3010    0.7450    0.9330];
set(groot,'DefaultAxesColorOrder', color);

% plot data
test11Curve = plot(Crosshead11, Load11);
test12Curve = plot(Crosshead12, Load12);

test21Curve = plot(Crosshead21, Load21);
test22Curve = plot(Crosshead22, Load22);

test31Curve = plot(Crosshead31, Load31);
test32Curve = plot(Crosshead32, Load32);

% headings
xlabel('Absolute Change in Length of Spring (mm)');
ylabel('Force Applied on Spring (N)');
title('Cyclic Testing: Immersed in Water');

% legend
legend([test11Curve, test21Curve, test31Curve], 'Trial 1', 'Trial 2', 'Trial
3', 'Location', 'northwest');

% fit bounds to data
axis([0 6 0 12]);
hold off;

```

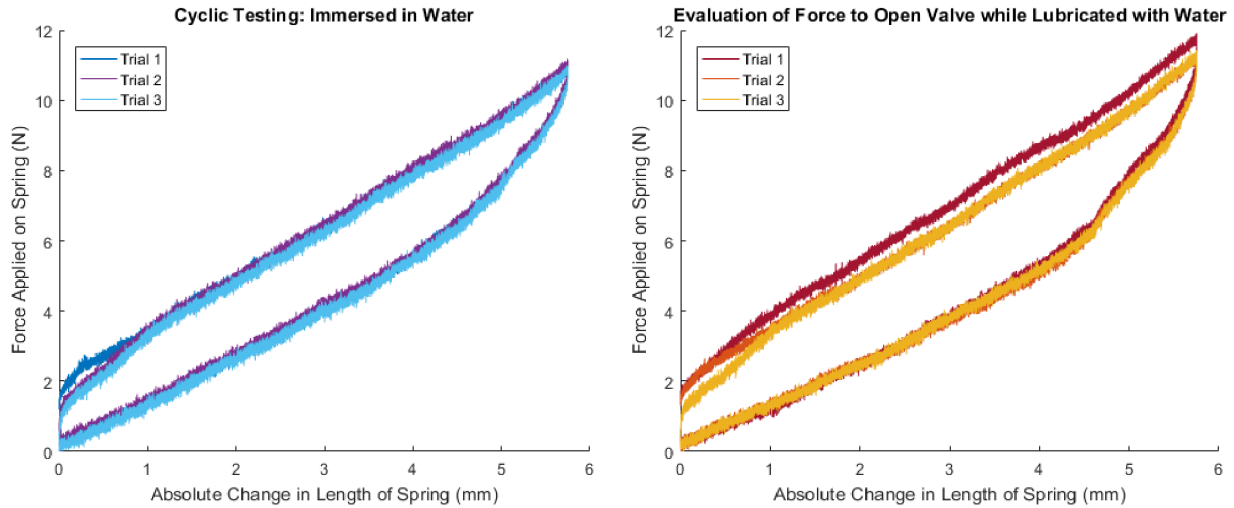


Figure 15. Graphs containing paths observed in cyclic load testing (by Catharine Flynn).

C.4. Graphical Comparison of Conditions

Two separate code files were created: one evaluating the data points while the piston was in cyclic loading and the other evaluating the data piston compressed to its maximum. The two programs are extremely similar. They only vary in the folders needed to access the data and the color scheme chosen to represent the data sets to better differentiate the outputs. While the program only outputs one figure of data, it was considered to be best to have both graphs for clarity.

```
%% Force Compare
% v 0.0
% April 27, 2017
% BME 301: shunt_valve
% Author: Catharine Flynn
% Team Members: Emma Alley, Karl Fetsch, Drew Miller
% By now, you can probably tell that I always write original code.

%% clear command window, close all windows, clear workspace
clc;
close all;
clear;

%% Summary of Test Parameters
% * testFile.data(:,1) Crosshead, the displacement of the MTS head (mm)
% * testFile.data(:,2) Load (N)
% * testFile.data(:,3) Time(s) The function (uuiimport) automatically
% sorts out the data from the header text. If not, the user can do that
% instead.

%% Import data
% dat = fullfile('myfolder','mysubfolder','myfile.txt')
```



```

% (subfolder may be omitted, can also use unlimited subfolders)
% 'DAQ- Crosshead, ... - (Timed).txt' -> 'DAQ- Crosshead, (Timed).txt'

% Immersed
datum = fullfile('ForceToOpenImmersed', 'dunkForcel', 'DAQ- Crosshead,
(Timed).txt');
structTest1 = uimport(datum);

% Lubricated
datum = fullfile('ForceToOpenLubricated', 'LubeForcel', 'DAQ- Crosshead,
(Timed).txt');
structTest2 = uimport(datum);

%% Assign variables
dblDisp1 = structTest1.data(:,1);
dblLoad1 = structTest1.data(:,2)+abs(structTest1.data(1,2));

dblDisp2 = structTest2.data(:,1);
dblLoad2 = structTest2.data(:,2)+abs(structTest2.data(1,2));

%% Plot data
figure;
hold all;    % plots everything on the same figure

% set colors for trials
color = [ 0 0.4470 0.7410
         0.6350 0.0780 0.1840];
set(groot,'DefaultAxesColorOrder', color)

% plot data
plot(dblDisp1, dblLoad1);
plot(dblDisp2, dblLoad2)

% headings
xlabel('Absolute Change in Length of Spring (mm)');
ylabel('Force Applied on Spring (N)');
title('Comparison of Force to Open Valve');

% legend
legend('Immersed', 'Lubricated', 'Location','northwest');

% fit bounds to data
axis([0 6 0 12]);
hold off;

```

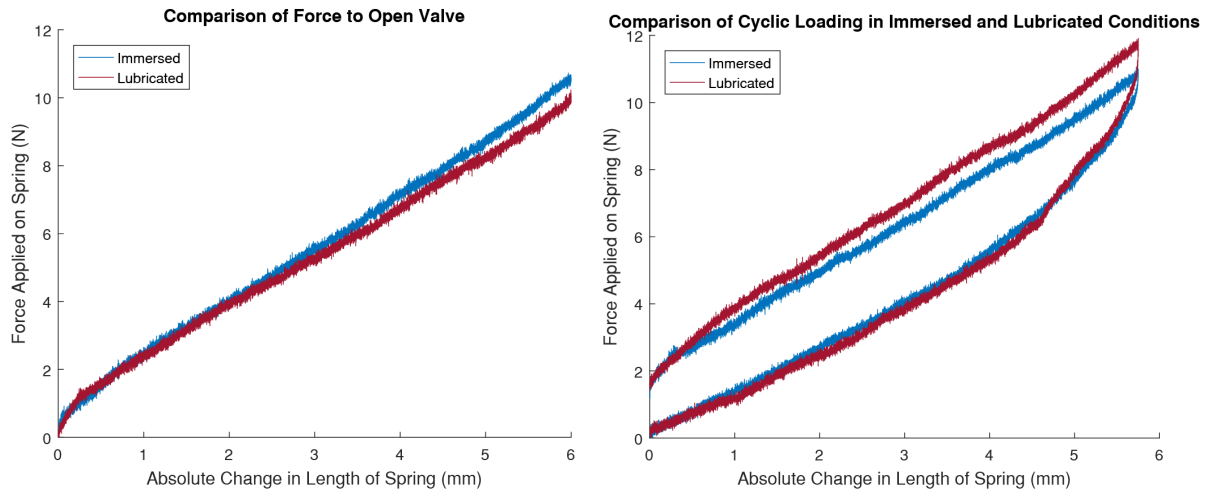


Figure 16. Graphical outputs comparing two trials of the different conditions (by Catharine Flynn).

D. Solidworks Engineering Drawing: Piston

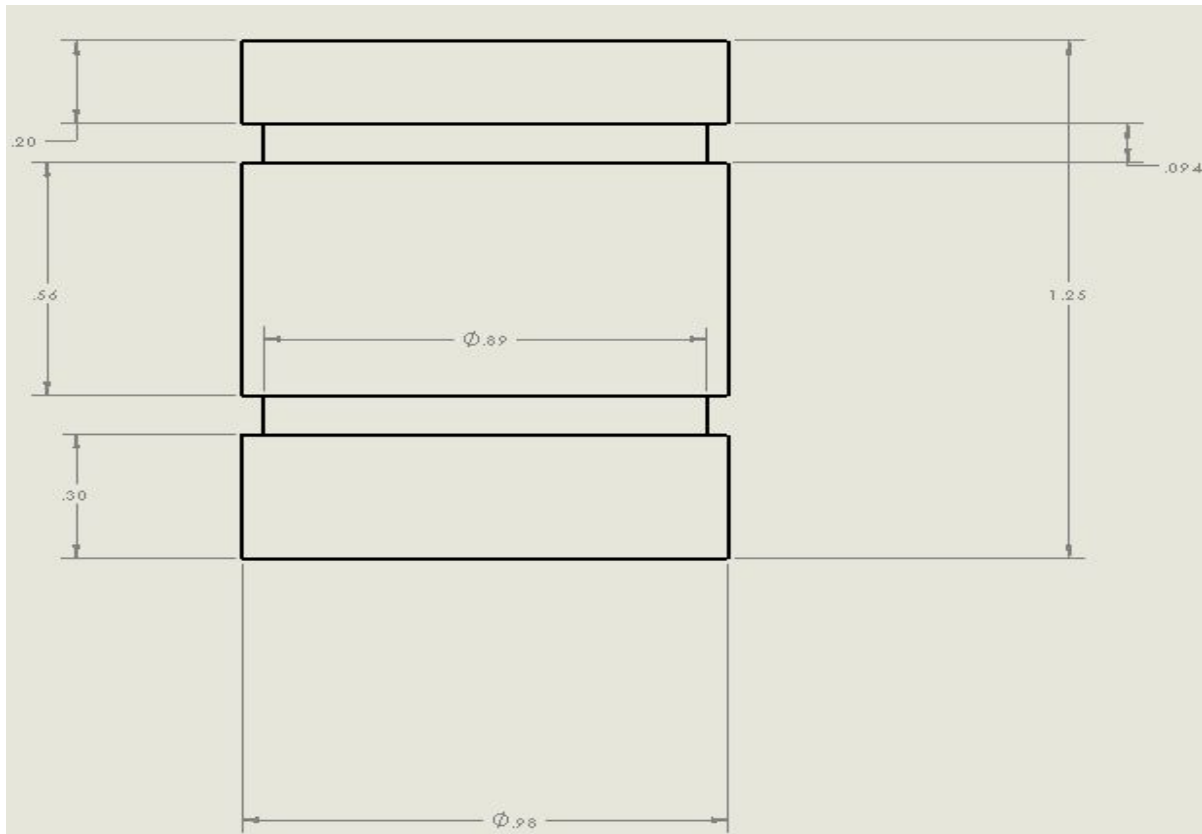


Figure 17. Solidworks generated engineering drawing of the final piston design with associated dimensions (by Drew Miller).